

PER/TIM-mediated amplification, gene dosage effects and temperature compensation in an interlocking-feedback loop model of the *Drosophila* circadian clock

Peter Ruoff^{a,*}, Melinda K. Christensen^a, Vijay K. Sharma^b

^aFaculty of Science and Technology, University of Stavanger, N-4036 Stavanger, Norway

^bChronobiology Laboratory, Evolutionary & Organismal Biology Unit, Jawaharlal Nehru Centre for Advanced Scientific Research, P.O. Box. 6436, Jakkur, Bangalore 560064, Karnataka, India

Received 28 October 2004; received in revised form 28 February 2005; accepted 29 March 2005

Available online 1 June 2005

Abstract

We have analysed a first-order kinetic representation of an interlocking-feedback loop model for the *Drosophila* circadian clock. In this model, the transcription factor *Drosophila* CLOCK (dCLK) which activates the clock genes *period* (*per*) and *timeless* (*tim*) is subjected to positive and negative regulations by the proteins ‘PAR Domain Protein 1’ (PDP1) and VRILLE (VRI), whose transcription is activated by dCLK. The PER/TIM complex binds to dCLK and in this way reduces the activity of dCLK. The results of our simulations suggest that the positive and negative feedback loops of *Pdp1* and *vri* are essential for the overall oscillations. Although self sustained oscillations can be obtained without *per/tim*, the model shows that the PER/TIM complex plays an important role in amplification and stabilization of the oscillations generated by the *Pdp1/vri* positive/negative feedback loops. We further show that in contrast to a single (*per/tim*) negative feedback loop oscillator, the interlocking-feedback loop model can readily account for the effect of gene dosages of *per*, *vri*, and *Pdp1* on the period length. Calculations of phase resetting on a temperature compensated version of the model shows good agreement with experimental phase response curves for high and low temperature pulses. Also, the partial losses of temperature compensation in *per^S* and *per^L* mutants can be described, which are related to decreased stabilities of the PER/TIM complex in *per^S* and the stronger/more stable inhibitory complex between dCLK and PER/TIM in *per^L*, respectively. The model shows (somewhat surprisingly) poor entrainment properties, especially under extended light/dark (L/D) cycles, which suggests that parts of the L/D tracking or sensing system are not well represented.

© 2005 Elsevier Ltd. All rights reserved.

Keywords: Circadian oscillations; *Drosophila*; Temperature compensation; Gene dosage; Interlocking-feedback loop; Molecular amplification; PDP1; VRILLE; PERIOD; TIMELESS

1. Introduction

Circadian rhythms (Bünning, 1963; Dunlap et al., 2003; Edmonds, 1988) play important roles in the adaptation of organisms to their environments. They act as physiological clocks and exhibit homeostasis of the circadian period against environmental variations such as in temperature, pH, or nutrients (Pittendrigh,

1993; Pittendrigh and Caldarola, 1973). The use of molecular genetic tools have helped to identify clock genes such as *period* (*per*) (Konopka and Benzer, 1971; Rosbash et al., 2003) and *frequency* (*freq*) (Feldman and Hoyle, 1973; Froehlich et al., 2003) in *Drosophila* and *Neurospora*, respectively.

A common element in the mechanisms of circadian rhythms is the presence of negative feedback loops (Dunlap, 1999). Recently, however, positive feedback loops have also been identified (Cyran et al., 2003; Lee et al., 2000), which points to the possibility that, similar

*Corresponding author. Tel.: +47 51 83 1887; fax: +47 51 83 1750.
E-mail address: peter.ruoff@uis.no (P. Ruoff).

to chemical oscillators (Franck, 1980; Higgins, 1967), positive and negative feedback loops are both important for the generation and stability of circadian rhythms.

Computational models (Goldbeter, 2002) have the potential to provide insights into the cellular processes, environmental influences (such as temperature, light, pH, nutritional conditions), and other yet unexplored aspects of the circadian oscillator. Such models are capable of making (quantitative) predictions which can be tested experimentally. In recent years a variety of reaction kinetic models have been developed for model organisms such as *Drosophila* (Hong and Tyson, 1997; Leloup and Goldbeter, 2000; Smolen et al., 2004; Ueda et al., 2001), *Neurospora* (Gonze et al., 2000; Ruoff et al., 1999a,b, 2001; Smolen et al., 2003), mammals (Forger and Peskin, 2003; Leloup and Goldbeter, 2003), plants (Johnsson et al., 1973; Lillo and Ruoff, 1984; Luttmann, 2000; Neff et al., 1998), and other insects except *Drosophila* (Lewis, 1994). Among these the *Drosophila* circadian clock is most intensively studied: the basic mechanism involves the expression of the PERIOD (PER) and TIMELESS (TIM) proteins and the formation of a heterodimer (PER/TIM), which is then transported into the nucleus where it inhibits the transcription of PER and TIM by binding to their transcription factor dCLK.CYC, a heterodimer between dCLK and CYCLE (Lee et al., 1999). The CYC concentrations were found to be in excess over the dCLK concentrations suggesting that the activity of dCLK.CYC is determined by the amount of dCLK (Bae et al., 2000).

Recently, two additional feedback loops were identified as parts of the core circadian pacemaker in *Drosophila*. In one of the loops, VRILLE (VRI), a protein which is activated by dCLK.CYC was found to repress transcription of the *dClk* gene forming a negative feedback loop, while in another positive feedback loop the protein ‘PAR Domain Protein 1’ (PDP1) activates the transcription of *dClk*, which itself activates the transcription of *Pdp1* (Blau and Young, 1999; Glossop et al., 2003). Because of the presence of both positive (activatory) and negative (inhibitory) feedbacks which deviate from previously studied single negative feedback models, we were interested in investigating the possible roles of the positive and negative feedback loops in a model with respect to the generation and stabilization of circadian oscillations in *Drosophila*.

Here we show that a representation of the negative and positive feedback loops by (mostly) first-order processes suggests that the PER/TIM heterodimer with support from the *Pdp1* mediated positive feedback loop, acts as an amplifier and stabilizer for the *vri/Pdp1*-generated oscillations. In contrast to a single negative feedback oscillator, the interlocking-feedback loop model can easily account for *per* and *vri* gene dosage effects on the circadian period. While our work was in

progress, results from a corresponding model appeared (Smolen et al., 2004). Although our calculations agree in many aspects with those of Smolen et al. (2004), for example in *per* and *vri* gene dosage effects on the period, a significant difference exists with respect to the role of the PER/TIM complex as an oscillation amplifier and the importance of the *Pdp1*-based positive feedback loop for the stabilization of the oscillations.

2. Computational method

2.1. The model

Analogous to the Goodwin oscillator (Goodwin, 1965; Ruoff et al., 1996), transcription and translation processes in our model are represented as first-order processes (Eqs. (1)–(12)), with exception of reactions (1) and (17) (Fig. 1). The representation of the (enzyme-catalysed) processes by first-order reactions complies with the view that many enzymes in vivo are present in low concentrations and work in the first-order range of their respective substrates (Dixon et al., 1979). Non-linear terms are included only for the activation of *dClk* transcription (positive feedback) by PDP1 and the inhibition of *dClk* transcription (negative feedback) by VRI (Fig. 1). The respective cooperativities (Eq. (1)) are described by numbers m ($0 \leq m \leq 1$) and n ($1 \leq n \leq 6$). For the sake of simplicity, *per* and *tim* are described as one variable (*per/tim*) and a distinction between the cytosolic and nuclear forms of PER/TIM have not been made. The active nuclear form of VRI (VRI_n^*) inhibits the transcription of *dClk* while the active nuclear form of PDP1 ($PDP1_n^*$) activates *dClk* transcription. Because CYC is always present at much higher concentrations than dCLK (Bae et al., 2000), the transcription factor dCLK.CYC is represented by a active nuclear form of dCLK, i.e. $dCLK_n^*$. The genes *vri*, *Pdp1*, and *per/tim* are activated by $dCLK_n^*$, while $dCLK_n^*$ becomes inactive after binding to PER/TIM (Fig. 1). Because we consider in our model only nuclear proteins in their active forms (i.e. VRI_n^* , $PDP1_n^*$, and $dCLK_n^*$) no explicit mass balance between nuclear forms (which should include active and inactive species) and cytosolic forms is formulated. This is an analogous approach as taken earlier in the Goodwin model (Ruoff and Rensing, 1996). The model’s rate equations are as follows:

$$\frac{d[dClk - mRNA]}{dt} = k_1 [PDP1_n^*]^m \frac{K_d}{K_d + [VRI_n^*]^n} - k_9 [dClk - mRNA], \quad (1)$$

$$\frac{d[dCLK_c]}{dt} = k_2 [dClk - mRNA] - k_{23} [dCLK_c], \quad (2)$$

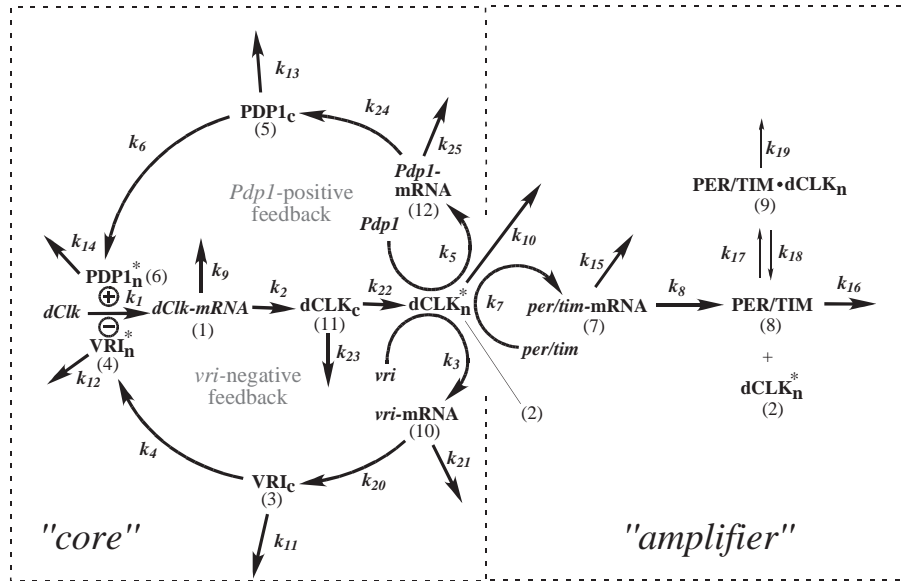


Fig. 1. Structure of the studied model. All reactions are first-order with exception of reactions (1) and (17). Reactions i (Table 2 and following tables) are those reactions with rate constant k_i . Reaction intermediate numbers j are given as numbers in parenthesis. Left (the “core”) part can show oscillations without involvement of PER/TIM ($k_7 = 0 \text{ h}^{-1}$). However, oscillations increase considerably in stability and amplitudes when expression of PER/TIM by $d\text{CLK}_n^*$ (the “amplifier”) is coupled to the core.

$$\begin{aligned} \frac{d[d\text{CLK}_n^*]}{dt} = & k_{22}[d\text{CLK}_c] - k_{10}[d\text{CLK}_n^*] \\ & - k_{17}[\text{PER}/\text{TIM}][d\text{CLK}_n^*] \\ & + k_{18}[\text{PER}/\text{TIM} \cdot d\text{CLK}_n^*], \end{aligned} \quad (3)$$

$$\frac{d[vri - mRNA]}{dt} = k_3[d\text{CLK}_n^*] - k_{21}[vri - mRNA], \quad (4)$$

$$\frac{d[\text{VRI}_c]}{dt} = k_{20}[vri - mRNA] - k_{11}[\text{VRI}_c], \quad (5)$$

$$\frac{d[\text{VRI}_n^*]}{dt} = k_4[\text{VRI}_c] - k_{12}[\text{VRI}_n^*], \quad (6)$$

$$\begin{aligned} \frac{d[pdp1 - mRNA]}{dt} = & k_5[d\text{CLK}_n^*] \\ & - k_{25}[pdp1 - mRNA], \end{aligned} \quad (7)$$

$$\begin{aligned} \frac{d[\text{PDP1}_c]}{dt} = & k_{24}[pdp1 - mRNA] \\ & - k_{13}[\text{PDP1}_c], \end{aligned} \quad (8)$$

$$\frac{d[\text{PDP1}_n^*]}{dt} = k_6[\text{PDP1}_c] - k_{14}[\text{PDP1}_n^*], \quad (9)$$

$$\begin{aligned} \frac{d[per/tim - mRNA]}{dt} = & k_7[d\text{CLK}_n^*] \\ & - k_{15}[per/tim - mRNA], \end{aligned} \quad (10)$$

$$\begin{aligned} \frac{d[\text{PER}/\text{TIM}]}{dt} = & k_8[per/tim - mRNA] \\ & - k_{16}[\text{PER}/\text{TIM}] \\ & - k_{17}[\text{PER}/\text{TIM}][d\text{CLK}_n^*] \\ & + k_{18}[\text{PER}/\text{TIM} \cdot d\text{CLK}_n^*], \end{aligned} \quad (11)$$

$$\begin{aligned} \frac{d[\text{PER}/\text{TIM} \cdot d\text{CLK}_n^*]}{dt} = & k_{17}[\text{PER}/\text{TIM}][d\text{CLK}_n^*] \\ & - (k_{18} + k_{19})[\text{PER}/\text{TIM} \cdot d\text{CLK}_n^*]. \end{aligned} \quad (12)$$

Eqs. (1)–(12) were solved numerically using the FORTRAN subroutine LSODE (Radhakrishnan and Hindmarsh, 1993).

For some of the results described later we found it more convenient to assign numbers to the different reaction intermediates. This assignment is shown in Table 1 and Fig. 1.

2.2. Control coefficients

Period and amplitude control (sensitivity) coefficients are defined as $C_i^P = \partial \ln P / \partial \ln k_i$ and $C_i^{A_j} = \partial \ln A_j / \partial \ln k_i$, where P is the oscillator’s period, and A_j and k_i are the amplitude of intermediate j and the rate constant of process i , respectively. The C_i^P and $C_i^{A_j}$ ’s are measures of the sensitivity of the oscillator’s period P or amplitude A_j upon changes of the rate constant k_i . Positive or negative control coefficients indicate that the period/amplitude increases or decreases, respectively, with an increase in k_i . To determine C_i^P or $C_i^{A_j}$ numerically, we

Table 1
Number assignment to reaction intermediates

Reaction intermediate number <i>j</i>	Name
1	<i>dClk</i> -mRNA
2	<i>dCLK_n</i> *
3	<i>VRI_c</i>
4	<i>VRI_n</i> *
5	<i>PDP1_c</i>
6	<i>PDP1_n</i> *
7	<i>per/tim</i> -mRNA
8	PER/TIM
9	PER/TIM <i>dCLK_n</i> *
10	<i>vri</i> -mRNA
11	<i>dCLK_c</i>
12	<i>Pdp1</i> -mRNA

first calculated the logarithm of the period/amplitude for different values of the rate constant k_i near a chosen reference point. In a final step C_i^P or C_i^{Aj} were obtained as the linear regression slopes of the $\ln P - \ln k_i$ or $\ln A_j - \ln k_i$ relationships. A numerical check of the calculated control coefficients can be made according to the summation theorems (Heinrich and Schuster, 1996; Ruoff et al., 2003):

$$\sum_i C_i^P = -1, \tag{13}$$

$$\sum_i C_i^{Aj} = 0. \tag{14}$$

However, it should be noted that the individual control coefficients depend on the values of the rate constants for a chosen reference state.

3. Results

3.1. *Pdp1*-positive feedback and PER/TIM-mediated amplification

The model can generate oscillations with period lengths within the circadian range and with relative phases of reaction intermediates that are close to experimentally observed values (Fig. 2). As indicated in Fig. 1, the model can be divided into two components, the “core” and the “amplifier”. The core segment consists of the *Pdp1* positive and *vri* negative feedback loops, which regulate the transcription of *dClk*, and are capable of generating sustained oscillations even in the absence of *per* ($k_7 = 0$, $n \geq 5$). A more or less arbitrarily chosen set of rate constants which shows sustained core oscillations is given in Table 2 (left columns). The C_i^{Aj} values (Table 3) indicate that *Pdp1*-mediated positive feedback (by increasing the values of k_5 , k_{24} or k_6) increases the amplitude of the *dClk*-

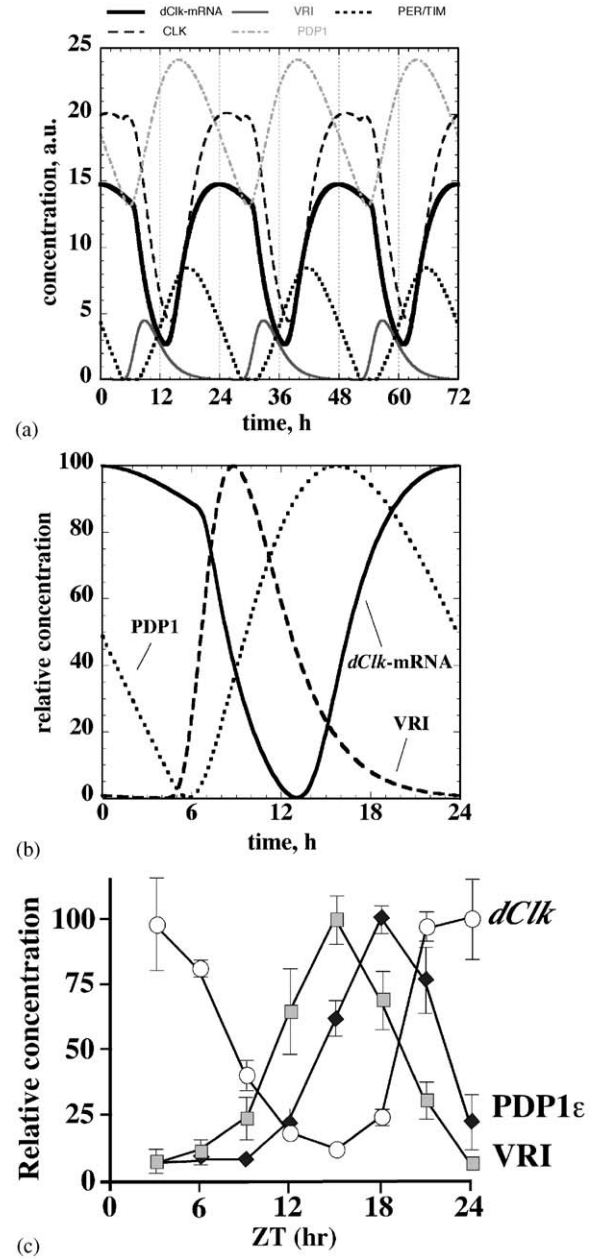


Fig. 2. (a) Concentration oscillation profiles for *dClk*-mRNA, PDP1 ($[PDP1]_c + [PDP1]_n$), CLK ($[dCLK]_c + [dCLK]_n$), VRI ($[VRI]_c + [VRI]_n$) and PER/TIM of complete model (core+amplifier). Rate constant and initial concentration values are given in Table 2. However, $k_1 - k_3$ were slightly increased (from 1.0 to 1.1 h^{-1}) to get a 24 h period length. (b) Scaled concentration profiles for the oscillations shown in Fig. 2a for *dClk*-mRNA, PDP1 and VRI. (c) Experimental concentration profiles of *dClk* (*dClk*-mRNA), PDP1 and VRI replotted from Cyran et al. (2003).

mRNA core oscillations, while promoting the *vri*-mediated negative feedback decrease the *dClk*-mRNA amplitudes. Fig. 3a illustrates the amplification effect of the positive feedback for core oscillations ($k_7 = 0 h^{-1}$, $n = 5$). At $t = 200 h$, k_6 is increased from 1 to 100 h^{-1} . As expected from the C_6^{A1} value (Table 3), the amplitude

Table 2
Rate constants and C_i^p values for core and complete model

Reaction i	Core model ^a		Complete model ^b	
	Value of k_i (h^{-1})	C_i^p	Value of k_i (h^{-1})	C_i^p
1	1	0.018	1	0.869
2	1	0.036	1	0.869
3	1	0.000	1	0.434
4	1	0.018	1	0.434
5	1	0.000	1	0.432
6	1	0.000	1	0.434
7	0	—	1	-0.819
8	1	0.000	1	-0.821
9	0.3	-0.196	0.3	-0.893
10	0.3	-0.196	0.3	-0.18
11	0.7	-0.143	0.7	-0.43
12	0.7	-0.179	0.7	-0.43
13	0.2	-0.018	0.2	-0.544
14	0.2	-0.036	0.2	-0.541
15	—	—	0.04	0.437
16	—	—	0.05	-0.128
17 ^c	—	—	1×10^6	0.002
18	—	—	0.01	-0.002
19 ^d	—	—	$1.0-1 \times 10^6$	0
20	2	0.036	2	0.434
21	0.4	-0.196	0.4	-0.392
22	0.1	0.036	0.1	0.869
23	0.8	-0.161	0.8	-0.924
24	1	0.018	1	0.434
25	0.1	-0.036	0.1	-0.544
	Period = 28.0 h	$\sum_i C_i^p = -1.000$	Period = 21.1 h	$\sum_i C_i^p = -0.996$

^aInitial concentrations for core oscillations: $[dClk\text{-mRNA}] = 6.0470$, $[dCLK_n^*] = 0.40639$, $[VRI_c] = 0.80317$, $[VRI_n^*] = 1.1364$, $[PDP1_c] = 24.5861$, $[PDP1_n^*] = 161.956$, $[vri\text{-mRNA}] = 0.40448$, $[dCLK_c] = 4.2548$, $[Pdp1\text{-mRNA}] = 3.4214$, $K_d = 1.0$, $n = 5$, $m = 0.5$.

^bInitial concentrations for complete model oscillations: $[dClk\text{-mRNA}] = 1.172e+1$, $[dCLK_n] = 6.815e-7$, $[VRI_c] = 1.203e-2$, $[VRI_n^*] = 3.839e-2$, $[PDP1_c] = 1.973$, $[PDP1_n^*] = 12.64$, $[per/tim\text{-mRNA}] = 0.9686$, $[PER/TIM] = 2.106$, $[PER/TIM.dCLK_n^*] = 1.435e-6$, $[vri\text{-mRNA}] = 1.822e-3$, $[dCLK_c] = 14.35$, $[Pdp1\text{-mRNA}] = 0.2412$, $K_d = 1.0$, $n = 5$, $m = 0.5$.

^cReaction (17) is a second-order process with dimension $[\text{conc (a.u.)}]^{-1}\text{h}^{-1}$.

^d k_{19} can vary over several orders of magnitude without significantly affecting the oscillator's period.

of the *dClk-mRNA* oscillations increase as k_6 (or any other rate constants which promotes the positive feedback loop) is increased.

In the complete model consisting of the core and the amplifying part, the $dCLK_n^*$ -induced expression of PER/TIM couples with the core by binding to $dCLK_n$ and thus decreasing its concentration. This removal of $dCLK_n^*$ by PER/TIM results in a dramatic increase in amplification by the *Pdp1*-positive feedback loop. Table 4 shows that promoting the positive feedback (by increasing k_5 , k_{24} or k_6) increases the amplitudes of all reaction intermediates. Fig. 3b shows the corresponding *dClk-mRNA* oscillations as in Fig. 3a for $t > 200$ h, but keeping k_6 constant to 100 h^{-1} for all t . At $t = 200$ h k_7 is increased from 0 to 1, which leads to a large increase in the amplitude of *dClk-mRNA*. Fig. 3c compares the *dClk-mRNA* amplitudes for core and complete model oscillations as a function of k_6 . Surprisingly, the amplitude control coefficients asso-

ciated with the negative feedback loop (i.e. C_3^{Aj} , C_{20}^{Aj} and C_4^{Aj}) have become positive! However, a closer inspection revealed that increasing k_3 , k_{20} or k_4 values lead to negative C_3^{Aj} , C_{20}^{Aj} and C_4^{Aj} values and never show the amplifying effects which are due to increasing values of the rate constants within the positive feedback loop (data not shown). This behavior shows that the control coefficients may change sign/value depending upon the values of the rate constants.

Removal of CLK_n^* by PER/TIM with increased k_{17} values leads to an increase in the *dClk-mRNA* amplitude with saturation at high k_{17} values (Fig. 4), which explains the low control coefficients for k_{17} values used (Tables 2 and 4). These results clearly demonstrate that the reason for the *dClk-mRNA* amplitude increase is the removal of CLK_n^* by PER/TIM (Fig. 4) through a coupling with the *Pdp1*-mediated positive feedback loop (Fig. 3).

Table 3

 $C_i^{A_j}$ values for core oscillations

i/j	1	2	3	4	5	6	10	11	12	$\sum_j C_i^{A_j}$
1	0.470	0.432	0.434	0.435	0.466	0.482	0.433	0.447	0.450	4.048
2	-0.524	0.437	0.441	0.443	0.476	0.494	0.438	0.453	0.458	3.116
3	-0.766	-0.783	0.218	0.220	-0.764	-0.756	0.218	-0.775	-0.773	-3.960
4	-0.765	-0.783	-0.781	0.220	-0.784	-0.783	-0.782	-0.776	-0.771	-6.004
5	0.238	0.220	0.222	0.222	1.235	1.242	0.221	0.228	1.231	5.060
6	0.242	0.223	0.224	0.225	0.241	1.251	0.223	0.230	0.234	3.093
9	0.605	0.362	0.256	0.234	0.037	-0.084	0.282	0.522	0.164	2.379
10	1.031	0.366	0.260	0.237	0.043	-0.076	0.286	0.990	0.168	3.305
11	0.343	0.335	-0.585	-0.602	0.157	0.070	0.317	0.347	0.226	0.609
12	0.348	0.341	0.311	-0.596	0.173	0.091	0.321	0.352	0.232	1.573
13	-0.309	-0.284	-0.286	-0.287	-0.747	-0.758	-0.285	-0.293	-0.298	-3.546
14	-0.311	-0.287	-0.288	-0.290	-0.316	-0.763	-0.288	-0.297	-0.302	-3.141
20	-0.763	-0.785	0.216	0.217	-0.785	-0.785	-0.784	-0.778	-0.775	-5.022
21	0.694	0.634	-0.147	-0.170	0.387	0.271	-0.121	0.672	0.502	2.722
22	-0.528	0.432	0.436	0.438	0.469	0.486	0.433	-0.553	0.451	2.063
23	0.081	-0.775	-0.842	-0.859	-1.026	-1.124	-0.825	-0.682	-0.929	-6.981
24	0.234	0.215	0.215	0.216	1.235	1.244	0.215	0.222	0.224	4.020
25	-0.323	-0.299	-0.301	-0.303	-0.496	-0.508	-0.300	-0.309	-0.491	-3.331
$\sum_i C_i^{A_j}$	-0.003	0.001	0.002	0.003	0.001	-0.004	0.002	0.001	0.000	$\sum_{i,j} C_i^{A_j} = 0.003$

Index i (columns) identifies the reactions, index j (rows) identifies the reaction intermediates (see Fig. 1, Table 1). Rate constant values are given in Table 2.

3.2. PER/TIM-mediated stabilization of oscillations: importance of the positive and negative feedback loops

The coupling of PER/TIM to the core not only increase the amplitude of *dClk*-mRNA oscillations but also makes the oscillator much more robust with respect to variations in the VRI_n^* cooperativity n (Eq. (1)). Even for n -values as low as 1 the model generates sustained oscillations. Fig. 3d shows the behavior of the system as in Fig. 3b, but the value of n was reduced from 5 to 1. Now the core is no longer able to show sustained oscillations, while the complete model still shows large amplitude oscillations. This suggests that the *per* gene not only plays a crucial role in regulating the oscillator's amplitudes but is also important for the oscillator's stability/robustness.

Although our simulations show that the *Pdp1*-mediated positive feedback loop plays an important role in terms of promoting and stabilizing the oscillations, both positive and negative feedback loops are necessary to generate oscillations, at least for the parameter values used in this study. The model was unable to generate oscillations when one of the rate constants within the positive (or negative) feedback loop was set to zero (or were very small), even for n values as high as 11 (data not shown).

3.3. Effect of gene dosage and rate constants on period length

Smith and Konopka (1982) found that the period length of the *Drosophila* circadian rhythm is shortened

when the gene dosage at the *per* locus is increased. While this behavior is not easily modeled with a single negative feedback oscillator (as indicated by the control coefficients for the Goodwin oscillator; see Ruoff and Rensing, 1996), the present model can readily account for *per* dosage effects as described in Table 2 and Fig. 5a. In Fig. 5a experimental *per* gene dosage data (Cote and Brody, 1986) are compared with data obtained from our model. Calculations show that the period length decreases with increasing k_7 values, which reflect increasing *per* gene dosage. In relating k_7 with *per* gene dosage, a power-law relationship between rate constant k_7 and the *per* (in our model *per/tim*) dosage is considered, i.e.

$$k_7 = a(\text{dose of } per/tim)^b. \quad (15)$$

Choosing $a = 6$ and $b = 0.131$ ($k_6 = 60 \text{ h}^{-1}$) the calculated period length (open circles in Fig. 5a) match closely the experimental data (solid squares and cross). By increasing k_6 , we found that the slope of the period length vs. k_7 relationship becomes less negative, which means that for different k_6 values the model still can describe the experimental *per* dosage data, but with different values of a and b (Eq. (15)).

Blau and Young (1999) observed that reducing the dosage of *vri* shortened the period of the flies' activity rhythm. This finding is in agreement with the model, which predicts robust oscillations and an increase/decrease in the period when the transcription rate (gene dosage) of *vri* is increased/decreased (Table 2,

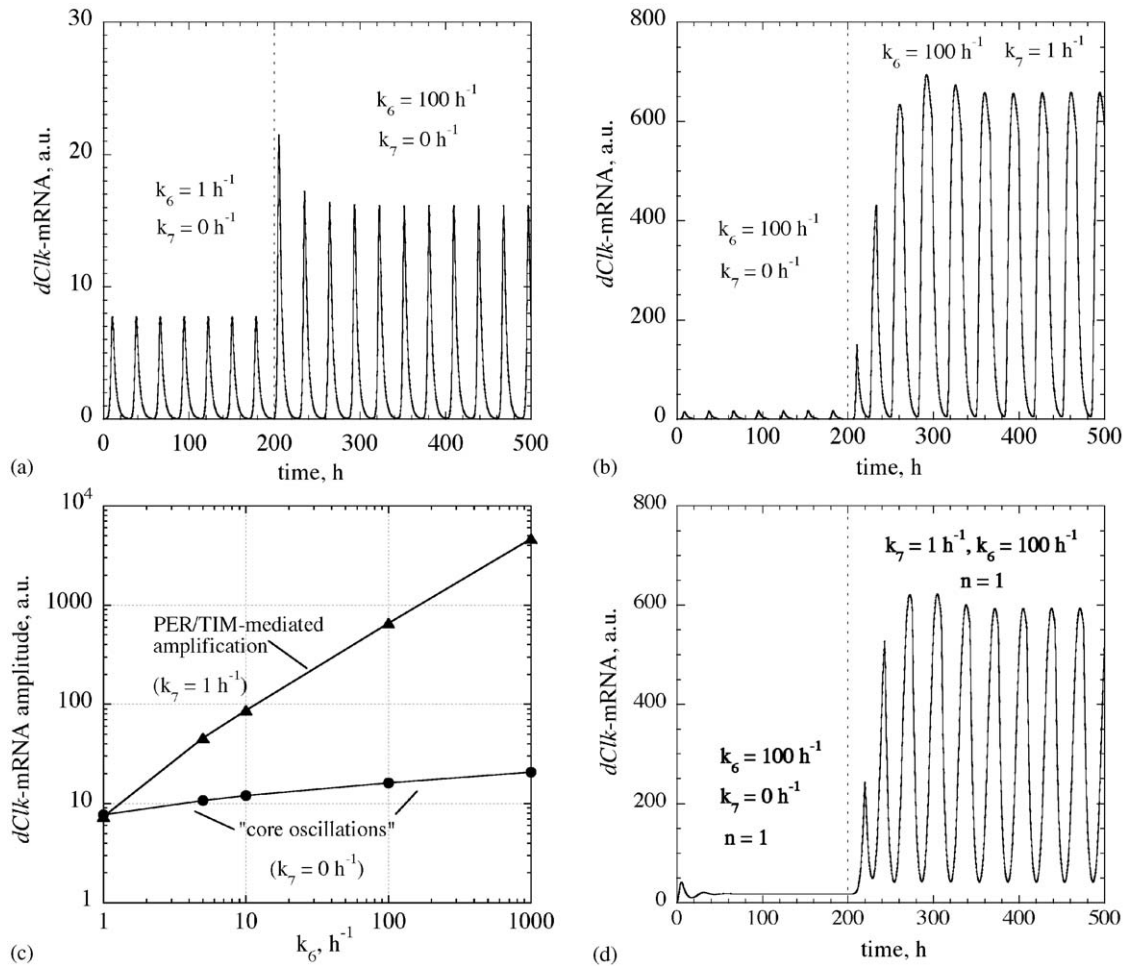


Fig. 3. PER/TIM-mediated amplification of oscillations through the *Pdp1*-positive feedback loop. (a) Increase of *dClk*-mRNA amplitude of core oscillations when k_6 is increased from 1 to 100 h^{-1} at $t = 200 \text{ h}$. (b) The amplitude increase in Fig. 3a is dramatically amplified when *per/tim* expression is coupled to the core by setting $k_7 = 1 \text{ h}^{-1}$ at $t = 200 \text{ h}$ (keeping k_6 constant at 100 h^{-1} for all t). (c) Comparison of the *dClk*-mRNA amplitude increase as a function of k_6 between PER/TIM-mediated amplification ($k_7 = 1 \text{ h}^{-1}$) and the *Pdp1*-induced increase of *dClk*-mRNA amplitude in core oscillations ($k_7 = 0 \text{ h}^{-1}$). (d) For $n = 1$ (Eq. (1)) no core oscillations are observed, but coupling the *per/tim* expression with the core ($k_7 = 1 \text{ h}^{-1}$) shows stable, large amplitude oscillations (k_6 is kept constant at 100 h^{-1}). Initial concentrations and rate constant values are those given in Table 2, unless otherwise stated in the figures.

Fig. 5b). In accordance with the C_5^P control coefficient (Table 2, complete model), the model also predicts that the period length should depend on *Pdp1* gene dosage more or less identical to the *vri* dosage (data not shown).

An important question is how circadian oscillations depend on the stabilities of key proteins. For example from studies of the Goodwin oscillator it was predicted that an increased/decreased FRQ protein stability should increase/decrease *Neurospora's* circadian period length, and should also alter temperature compensation of the clock (Ruoff et al., 1996, 1999b). Subsequent experiments showed that phosphorylation and kinase activities indeed play an important role in the stability of FRQ and in determining the period length of *Neurospora's* circadian clock (Liu et al., 2000). Similarly,

the Goodwin model was able to describe the altered periods in *Drosophila's per^S* and *per^L* clock mutants with their characteristic reciprocal behavior in temperature compensation (Konopka et al., 1989) in terms of altered stability of the PER protein and an altered PER–PER or PER–protein interaction (Ruoff et al., 1996). In particular, a decreased stability in PER protein predicted a shorter period (Ruoff et al., 1996), which appears to be related to the phosphorylation state of PER (Preuss et al., 2004; Rosbash et al., 2003). Also in the present model we found that an increase in the PER/TIM stability (i.e. a decrease in the rate constant k_{16}) results in an increased period length and a partial loss of the oscillator's temperature compensation (Table 2, see also next chapter). As indicated by the C_i^P coefficients, *Drosophila* mutants with increased

Table 4

$C_i^{A_j}$ values for oscillations of the complete model

i/j	1	2	3	4	5	6	7	8	9	10	11	12	$\sum_j C_i^{A_j}$
1	3.868	2.376	2.288	2.303	2.849	3.472	2.423	4.684	3.522	2.317	4.098	2.395	36.595
2	2.869	2.376	2.290	2.304	2.849	3.473	2.425	4.673	3.523	2.318	4.099	2.396	35.594
3	0.940	0.192	1.150	1.157	0.428	0.738	0.218	1.346	0.769	1.163	1.056	0.202	9.360
4	0.941	0.193	0.149	1.157	0.427	0.738	0.218	1.344	0.769	0.163	1.056	0.202	7.356
5	1.941	1.188	1.145	1.152	2.429	2.738	1.211	2.379	1.761	1.158	2.057	2.200	21.358
6	1.931	1.187	1.143	1.151	1.424	2.733	1.211	2.355	1.760	1.158	2.046	1.197	19.295
7	-2.749	-1.762	-2.129	-2.174	-2.689	-3.313	-1.237	-3.407	-2.313	-2.010	-2.969	-2.197	-28.948
8	-2.732	-1.757	-2.123	-2.167	-2.680	-3.276	-2.232	-3.361	-2.303	-2.004	-2.952	-2.190	-29.776
9	-3.303	-2.332	-2.273	-2.290	-2.851	-3.490	-2.410	-4.286	-3.181	-2.292	-3.537	-2.380	-34.625
10	-0.294	-0.271	-0.245	-0.246	-0.357	-0.487	-0.275	-0.588	-0.373	-0.265	-0.322	-0.272	-3.994
11	-0.790	-0.177	-0.798	-0.894	-0.415	-0.723	-0.206	-1.200	-0.667	-0.149	-0.910	-0.190	-7.119
12	-0.789	-0.178	-0.139	-0.893	-0.416	-0.724	-0.206	-1.200	-0.667	-0.150	-0.910	-0.190	-6.461
13	-2.078	-1.314	-1.281	-1.291	-1.941	-2.315	-1.364	-2.651	-1.948	-1.291	-2.211	-1.346	-21.031
14	-2.075	-1.314	-1.279	-1.289	-1.631	-2.316	-1.364	-2.636	-1.947	-1.289	-2.208	-1.344	-20.693
15	2.274	1.797	1.785	1.795	2.066	2.377	1.837	2.823	2.261	1.788	2.442	1.835	25.079
16	-0.069	-0.077	-0.061	-0.063	-0.144	-0.236	-0.082	-0.295	-0.037	-0.065	-0.079	-0.077	-1.285
17	0.000	0.000	0.000	0.000	0.000	0.001	0.000	-0.001	0.000	0.000	0.000	0.000	0.000
18	0.000	0.000	0.000	0.000	0.000	0.001	0.001	0.000	0.000	0.001	0.000	0.000	0.003
19	0.000	0.000	0.000	0.000	0.000	0.001	0.001	0.000	-1.000	0.000	0.000	0.000	-0.999
20	0.940	0.193	1.150	1.157	0.428	0.740	0.219	1.346	0.769	0.164	1.055	0.203	8.363
21	-0.648	-0.157	-0.592	-0.682	-0.377	-0.660	-0.185	-1.051	-0.561	-0.539	-0.764	-0.170	-6.386
22	2.867	2.375	2.289	2.304	2.848	3.472	2.424	4.669	3.522	2.317	3.096	2.395	34.578
23	-2.927	-2.422	-2.339	-2.355	-2.933	-3.596	-2.482	-4.664	-3.487	-2.365	-4.008	-2.451	-36.027
24	1.934	1.187	1.145	1.152	2.426	2.736	1.212	2.367	1.761	1.159	2.049	1.199	20.327
25	-2.047	-1.301	-1.272	-1.283	-1.741	-2.122	-1.355	-2.640	-1.927	-1.280	-2.179	-1.416	-20.563
$\sum_i C_i^{A_j}$	0.005	0.001	0.003	0.003	0.001	-0.039	0.005	0.007	0.007	0.004	0.005	0.000	$\sum_{ij} C_i^{A_j} = 0.001$

Index i (columns) identifies the 26 reactions, index j identifies the 12 reaction intermediates (Fig. 1, Table 1). Rate constant values are given in Table 2.

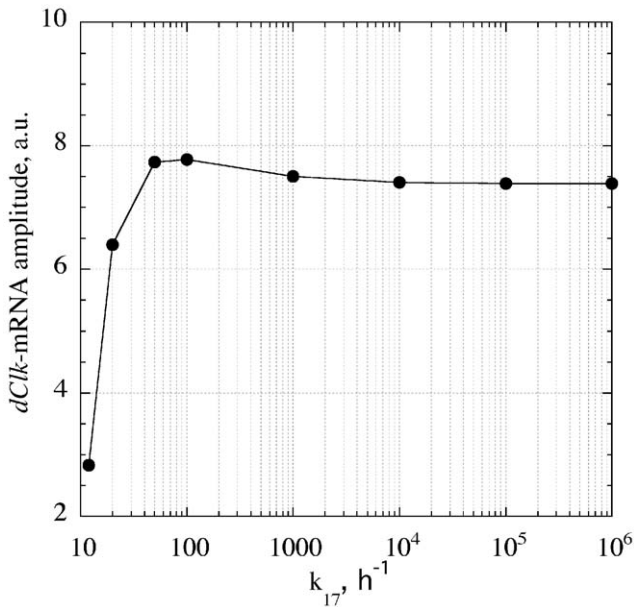


Fig. 4. The $dClk$ -mRNA amplitude shows saturation at high values of k_{17} , explaining the low $C_i^{A_{17}}$ values.

stabilities in VRI or PDP1 proteins should also show increased period lengths and an altered temperature compensation.

3.4. Influence of temperature and temperature compensation

Temperature is an important “Zeitgeber” for many circadian clocks (Rensing and Ruoff, 2002) while temperature compensation is an essential property of all circadian (and ultradian) clocks. Temperature compensation means that the oscillator’s period P is practically unchanged under different constant environmental temperatures, despite the fact that physiological component processes are generally quite dependent upon temperature (Ruoff et al., 2000). The condition for obtaining temperature compensation for a reaction kinetic oscillator is given by

$$RT^2 \frac{d \ln P}{dT} = \sum_j \frac{\partial \ln P}{\partial \ln k_j} E_j + \sum_l \frac{\partial \ln P}{\partial \ln K_l} \Delta H_l^0 = 0, \tag{16}$$

where k_i are rate constants and K_l are equilibrium constants of any rapid equilibrium which might have been established in the system. The temperature dependence of the rate constants are usually described by the Arrhenius equation (Laidler and Meiser, 1995)

$$k_j = A_j \exp(-E_j/RT), \tag{17}$$

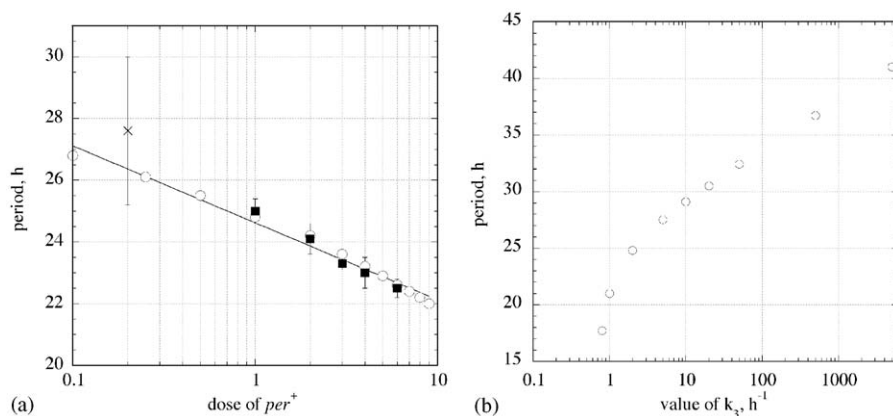


Fig. 5. (a) Effect of *per* (*per/tim*) dosage on the period. Calculated values are represented by open circles, while experimental values are shown as solid squares and a cross (replotted from Cote and Brody, 1986). Rate constant values are those of Table 2, except for *k*₆, which was taken as 60 h⁻¹. For this *k*₆ value, the relationship between *per/tim* dosage and *k*₇ is given by Eq. (15) (*a* = 6, *b* = 0.131). (b) Period length as a function of *k*₃. The relationship between *k*₃ and *vri* dosage may be described by a power-law similar to Eq. (15), but too few experimental data are presently available for a test. A practically identical relationship between period length and *k*₅ (relating to the dose of *PdpI*) was found (data not shown).

where E_j is the activation energy of process j , and A_j is the pre-exponential factor. R and T are the gas constant and temperature (in Kelvin), respectively. The activation energy and the pre-exponential factor in Eq. (17) vary generally little with temperature and are therefore often considered (as here) as temperature independent. In the case where rapid-equilibrium constants K_l are included in the rate equations, the temperature-dependence of K_l can be described in an analogous way as the Arrhenius equation, i.e. by substituting the activation energy by the enthalpy ΔH_l^0 . In this case the pre-exponential factor can still be treated as temperature-independent and becomes $A_l = \exp(-\Delta S_l^0/R)$. Because the C_i^P 's depend upon the rate constants k_j , the condition for temperature compensation becomes only approximately valid within a certain temperature range. For such a local temperature range the condition for temperature compensation can be formulated as (Ruoff, 1992, 2003)

$$\sum_i C_i^P E_i \cong 0. \quad (18)$$

It should be noted that there is, in principle, an infinite number of activation energy (E_i) combinations which for a given set of C_i^P values satisfies Eq. (18) and lead to temperature compensation. Because activation energies are always positive, Eq. (18) requires (in addition to Eq. (13)) that some of the C_i^P 's are also positive. Although Eq. (13) opens the possibility that all C_i^P 's could be negative (which would not allow any form of temperature compensation by Eq. (18)), so far, in all reaction kinetic oscillator models investigated, both positive and negative C_i^P 's have been found.

Small changes in the rate constants k_1 – k_3 (Table 2) from 1.0 to 1.1 h⁻¹ result in oscillations with a period close to 24 h (Fig. 2a). This set of rate constants has been used as a starting point to investigate temperature

compensation in the model. In order to apply Eq. (18), we have to first define a reference temperature T_{ref} , for which the chosen set of rate constants designated as $\{k_j^{chosen}\}$ applies. In the next step, the A_j values are determined as $A_j = k_j^{chosen} \exp(E_j/RT_{ref})$ and substituted into Eq. (17), from which the rate constants can be calculated for a desired temperature T .

Before investigating temperature compensation, we were interested in studying the temperature dependence of the period under a situation where all activation energies assume the same value. Curve 1 in Fig. 6a (gray diamonds) shows how the period length of the oscillations shown in Fig. 2a decreases with increasing temperature when all the activation energies are set to 30 kJ/mol. The T_{ref} was set to 25 °C; at this temperature the oscillator shows, as expected, a period of about 24 h (Fig. 2a). In the light of Eq. (13), the period decreases with increasing temperature because all activation energies are considered to be equal ($E_i = 30$ kJ/mol) leading to $\sum_i C_i^P E_i = -30$ kJ/mol. In fact, an Arrhenius plot, i.e. plotting the inverse of the period vs. $1/T$ (Laidler and Meiser, 1995), would have a slope ($-E_a/R$) with an overall activation energy E_a of 30 kJ/mol (data not shown). Such a strong decrease of the period with increasing temperature is often experimentally observed in chemical oscillators, for example in the Belousov–Zhabotinsky reaction (Nagy et al., 1996; Ruoff, 1995). It reflects the situation that activation energies of the underlying component processes in chemical oscillators are randomly distributed (and not subject to evolutionary mutation and selection mechanisms as in biological clocks) which gives dP/dT (according to Van't Hoff's rule) a large negative value. Interestingly, the condition of temperature compensation in chemical oscillators have recently been experimentally studied (Kóvacs and Rábai, 2002; Rábai and Hanazaki, 1999),

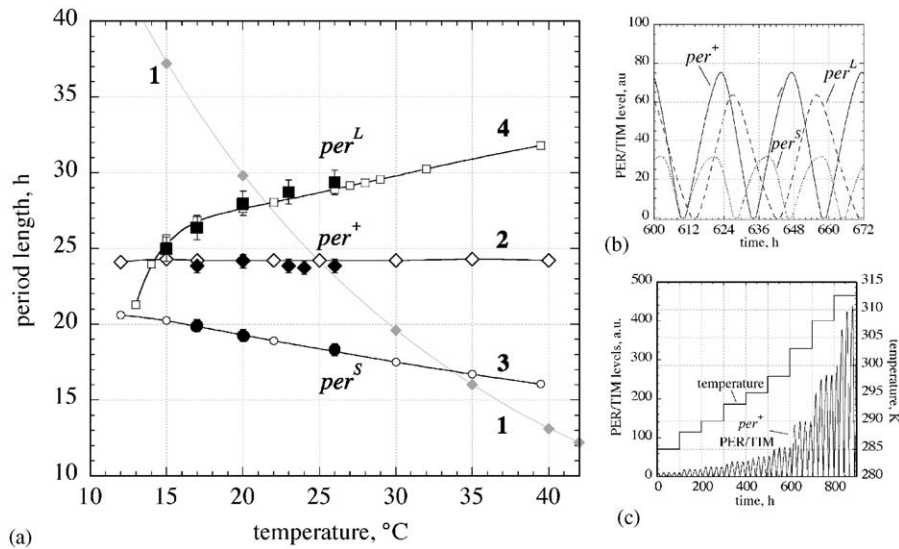


Fig. 6. (a) Period length as a function of temperature with different rate constant parameters and activation energies. (1) Calculated period dependence (gray curve and diamonds) when rate constant values are those used as in Fig. 2a (Table 2, with k_1-k_3 increased from 1.0 to 1.1 h^{-1} , $T_{\text{ref}} = 25^\circ\text{C}$) and all activation energies were 30 kJ/mol. (2) Calculated temperature compensation (open diamonds) showing per^+ behavior (for parameter values, see Table 5). Experimental values are shown as solid diamonds. (3) Calculated temperature behavior of oscillations (open circles) showing per^S behavior (for parameter values, see Table 5). Experimental values are shown as solid circles. (4) Calculated temperature behavior of oscillation showing per^L behavior (open squares; for parameter values, see Table 5). Experimental values are shown as solid squares. All experimental values were redrawn from Konopka et al. (1989). (b) Amplitude levels of calculated PER/TIM oscillations for per^+ , per^S , and per^L parametrizations (Table 5). Note the lower PER/TIM amplitude in per^S compared with the PER/TIM oscillations in per^+ and per^L . (c) PER/TIM levels increase as a function of absolute temperature ($T(\text{K}) = 273.15\text{ K} + \text{degrees}^\circ\text{C} \times (1\text{ K}/^\circ\text{C})$ for the temperature compensated per^+ parametrization (Table 5).

and the results are in close accordance with the principle of opposing reactions as described by Eq. (18).

In search for activation energy combinations which result in temperature compensation over a larger temperature range, we used a “stochastic fitting method”. In this method we started with the set of rate constant values shown in Table 5 (column per^+) defined at 11°C , where all activation energies are initially given a value of 30 kJ/mol. During an iterative procedure a randomly chosen activation energy value (up to a maximum of 60 kJ/mol) is then assigned to a randomly chosen rate constant (reaction). Rate constants (by applying Eq. (17)) and periods then are calculated for different temperatures T_i within a given temperature interval. The calculated periods $P_{\text{calc}}(T_i)$ are compared with a pre-defined target function $P_{\text{target}}(T_i)$. The deviation DEV between the calculated and pre-defined period values

$$DEV = \sqrt{\frac{\sum_{i=1}^N (P_{\text{calc}}(T_i) - P_{\text{target}}(T_i))^2}{N}} \quad (19)$$

is evaluated by Eq. (19), where N is the number of temperature points within the temperature interval. Once a randomly selected rate constant gives a lower DEV compared with previously calculated DEV values, the previous activation energy for this rate constant is replaced by the new one, and is updated again when a

new random selection leads to an even lower DEV value. Curve 2 (Fig. 6) shows an example for an activation energy combination (Table 5) leading to temperature compensated oscillations when $P_{\text{target}}(T_i) = 24\text{ h}$ (for all T_i), exhibiting *wild type* (per^+) behavior. Curves 3 and 4 show the period length as a function of temperature when activation energies and rate constants in the per/tim expression pathways of the temperature compensated set (curve 1) are changed (Table 5, grayed entries), resembling per^L and per^S behavior, respectively. The experimental data on the period lengths as a function of temperature for the per^+ , per^S , and per^L mutant flies are shown as solid points (Konopka et al., 1989). The model predicts (Table 5, outlined) that the per^S mutation (Yu et al., 1987) is associated with an increased turnover and increased temperature sensitivity (increased E_{16}) of PER/TIM. For the per^L temperature response behavior, the model suggests (Table 5, grayed entries in right columns) that several processes in the PER/TIM expression pathway might be affected by the per^L mutation (Huang et al., 1995), but the largest change appears to be due to a reduction in the stability of the PER/TIM.dCLK_n complex (decrease of k_{17}) accompanied by an increase in its temperature sensitivity (increase of E_{17}). The calculated $\sum C_i^p E_i$ values for per^+ , per^S and per^L parametrizations are also shown in Table 5. Similar predictions for the per^L and per^S temperature behaviors have earlier been made using the Goodwin oscillator (Ruoff et al., 1996). Fig. 6b shows

Table 5

Values of rate constants, activation energies and control coefficients describing per^+ , per^S , and per^L behaviors^a

Reaction <i>i</i>	k_i (per^+) (h^{-1})	E_i (per^+) (kJ/mol) ^b	C_i^P (per^+) (25 °C)	$C_i^P E_i$ (per^+) (kJ/mol) (25 °C)	k_i (per^S) (h^{-1})	E_i (per^S) (kJ/mol) ^b	C_i^P (per^S) (25 °C)	$C_i^P E_i$ (per^S) (kJ/mol) (25 °C)	k_i (per^L) (h^{-1})	E_i (per^L) (kJ/mol) ^b	C_i^P (per^L) (25 °C)	$C_i^P E_i$ (per^L) (kJ/mol) (25 °C)
1	1.1	58.8	0.144	8.469	1.1	58.8	0.190	11.186	1.1	58.8	0.157	9.210
2	1.1	20.6	0.165	3.399	1.1	20.6	0.163	3.360	1.1	20.6	0.157	3.226
3	1.1	31.0	0.103	3.193	1.1	31.0	0.082	2.528	1.1	31.0	0.087	2.695
4	1.0	46.6	0.103	4.800	1.0	46.6	0.082	3.802	1.0	46.6	0.070	3.241
5	1.0	43.3	0.062	2.680	1.0	43.3	0.082	3.527	1.0	43.3	0.070	3.011
6	1.0	26.9	0.103	2.775	1.0	26.9	0.109	2.931	1.0	26.9	0.070	1.875
7	1.0	39.2	-0.144	-5.645	1.0	39.2	-0.163	-6.400	0.85	19.6	-0.104	-2.049
8	1.0	27.3	-0.144	-3.927	1.0	27.3	-0.190	-5.189	1.3	14.6	-0.104	-1.522
9	0.3	1.7	-0.227	-0.377	0.3	1.7	-0.163	-0.271	0.3	1.7	-0.278	-0.462
10	0.3	18.1	-0.062	-1.120	0.3	18.1	-0.054	-0.984	0.3	18.1	-0.052	-0.944
11	0.7	33.3	-0.144	-4.801	0.7	33.3	-0.136	-4.531	0.7	33.3	-0.139	-4.641
12	0.7	5.4	-0.186	-1.004	0.7	5.4	-0.218	-1.183	0.7	5.4	-0.191	-1.041
13	0.2	59.1	-0.103	-6.089	0.2	59.1	-0.109	-6.432	0.2	59.1	-0.104	-6.172
14	0.2	28.3	-0.124	-3.503	0.2	28.3	-0.136	-3.839	0.2	28.3	-0.139	-3.932
15	0.04	19.4	-0.062	-1.198	0.04	19.4	-0.082	-1.579	0.02	12.9	0.035	0.449
16	0.05	0.6	-0.144	-0.086	<i>0.13</i>	35.0	-0.218	-7.613	0.019	0.7	-0.035	-0.023
17 ^c	1×10^6	13.1	0.000	0.000	1×10^6	13.1	0.000	0.000	80.0	27.1	0.000	0.000
18	0.01	23.2	0.000	0.000	0.01	23.2	0.000	0.000	0.01	23.2	0.000	0.000
19	1.0	26.8	0.000	0.000	1.0	26.8	0.000	0.000	1.0	26.8	0.000	0.000
20	2.0	29.0	0.103	2.989	2.0	29.0	0.082	2.369	2.0	29.0	0.087	2.526
21	0.4	6.1	-0.289	-1.772	0.4	6.1	-0.299	-1.833	0.4	6.1	-0.313	-1.919
22	0.1	38.9	0.144	5.602	0.1	38.9	0.163	6.340	0.1	38.9	0.157	6.087
23	0.8	28.7	-0.206	-5.912	0.8	28.7	-0.218	-6.242	0.8	28.7	-0.209	-5.993
24	1.0	10.2	0.082	-0.218	1.0	10.2	0.082	0.830	1.0	10.2	0.052	0.531
25	0.1	1.1	-0.206	8.469	0.1	1.1	-0.163	-0.173	0.1	1.1	-0.313	-0.332
K_d	1.0	4.8	0.000	0.000	1.0	4.8	0.000	0.000	1.0	4.8	0.000	0.000
			$\sum_i C_i^P =$ -1.032	$\sum_i C_i^P E_i =$ -0.906			$\sum_i C_i^P =$ -1.115	$\sum_i C_i^P E_i =$ -9.398			$\sum_i C_i^P =$ -1.044	$\sum_i C_i^P E_i =$ 3.821

^aRate constant values are given for $T_{ref} = 284$ K (11 °C), $n = 5$, $m = 0.5$. All C_i^P values were calculated for 298 K (25 °C). E_i values are truncated to one digit after decimal point.

^bThe following initial concentrations of the reaction intermediates 1–12 (Table 1) can be used: 3.00237E+00, 1.45212E-07, 8.05907E-01, 1.73929E+00, 4.63242E+00, 1.75926E+01, 1.95971E+00, 4.20025E+00, 6.09918E-07, 1.44872E-01, 6.09917E+00, 9.14529E-01.

^cReaction (17) is a second-order process where k_{17} has the dimension [conc (a.u.)]⁻¹h⁻¹.

the PER/TIM oscillations of per^+ , per^S , and per^L parametrizations at 25 °C (298 K). Fig. 6c shows that the PER/TIM amplitude of the temperature compensated per^+ parametrization increases with increasing temperature, which is in agreement with the amplitude model (Lakin-Thomas et al., 1991). In the amplitude model temperature compensation is ensured by an increase in the amplitude of oscillation: although the velocity of the oscillator’s trajectory in phase space increases with increase in temperature, an increase in amplitude compensates for the increased velocity in phase space such that the period remains unaltered. Although the predicted amplitude effects (Lakin-Thomas et al., 1991) have been observed in other temperature compensated reaction kinetic oscillators (Ruoff, 1992; Ruoff et al., 2003), exceptions have been found theoretically as well as experimentally (Leloup and Goldbeter, 1999; Rensing and Ruoff, 2002; Ruoff et al., 2003).

3.5. Light/dark (L/D) entrainment and temperature pulse PRCs

Although periods of circadian rhythms are affected little by different constant temperature levels, their phases are sensitive to sudden temperature variations (steps or pulses) which lead to phase shifts. In *Drosophila* studies to estimate phase shift involve maintaining flies in L/D cycles (or in continuous light) before temperature pulses/steps are applied at different phases under constant darkness (DD) (Chandrasekaran, 1974; Zimmerman et al., 1968). A plot of the resulting phase shifts between unperturbed and perturbed rhythms as a function of the phase of perturbation defines a phase response curve (PRC). We have calculated the temperature pulse PRC of our model according to a protocol by Zimmerman et al. (1968). First, the rhythm is entrained to a L/D regime at 20 °C (or 28 °C), and then 12 h temperature pulses from 20 to

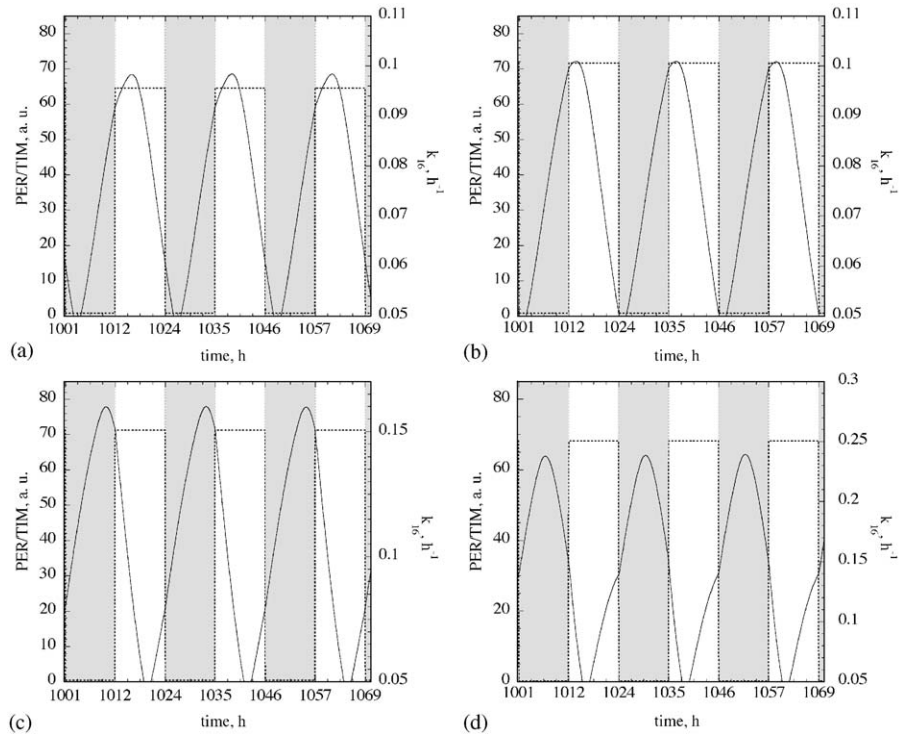


Fig. 7. Entrainment of the temperature compensated model (per^+ parametrization, Table 5) to 11.25:11.25 L/D cycles at 25°C. During light phases the degradation rate constant k_{16} of PER/TIM were increased by the following additional values: (a) 0.045 h^{-1} ; (b) 0.05 h^{-1} ; (c) 0.1 h^{-1} ; and (d) 0.2 h^{-1} (right-hand side ordinates). Start of the light phase (white areas) is described as Zeitgeber Time (ZT) 0, while start of the dark phase (dark areas) is ZT 12. Note the change in PER/TIM phase as the light-induced degradation of PER/TIM is altered.

28°C (or from 28 to 20°C) were applied at different phases of the rhythm in DD. Before we present the modeling of the temperature PRCs we briefly refer to the corresponding effects of light.

It has been shown experimentally that light increases the degradation of PER/TIM (Hunter-Ensor et al., 1996; Lee et al., 1996; Myers et al., 1996; Young et al., 1996; Zeng et al., 1996), a feature which has been used to model light responses and entrainment to L/D cycles (Klarsfeld et al., 2003; Leloup and Goldbeter, 1998; Smolen et al., 2004; Tyson et al., 1999). To model entrainment to L/D cycles we have (either at 20 or 28°C) increased the degradation rate constant of PER/TIM (k_{16}) during the light phase and restored its original dark value during the dark phase. The extent of increased PER/TIM degradation during light conditions were arbitrary chosen. Fig. 7 shows that the phase of PER/TIM changes relative to the L/D cycles is dependent upon the magnitude of PER/TIM removal during the light phase ($T = 25^\circ\text{C}$).

In order to model the temperature pulse PRCs we first imposed an L/D cycle at 20 or 28°C (other conditions were the same as those described in Fig. 7b) and then used 12 h temperature pulses, either a high temperature pulse (HTP, 20→28°C) or a low temperature pulse (LTP, 28→20°C), respectively, covering the subsequent dark phase after the LD→DD transition (which defines

circadian time 12; ct 12) for three cycles (72 h in DD). Surprisingly, the oscillator showed entrainment to L/D cycles only within a small window near its natural period, which is the reason for the 11.25:11.25 L/D entrainment scheme shown in Fig. 7. Figs. 8a, b show the results of the calculated HTP and LTP PRCs which match closely the experimental PRCs (Chandrasekaran, 1974; Zimmerman et al., 1968). The model is able to describe the characteristic behaviors of the HTP and LTP PRCs.

4. Discussion

4.1. Phase behavior of the Model

The aim of the present study was to investigate the roles of PER/TIM in connection with the *Pdp1* mediated positive and *vri* mediated negative feedback loops. In the present model we have deliberately taken (most of) the component processes as first-order reactions, in order to keep the model as simple as possible, and to also allow a comparison with previous results obtained with the Goodwin oscillator. The study of Kurosawa and coworkers on a single negative feedback oscillator showed that by introducing Michaelis–Menten kinetic terms within the model, the

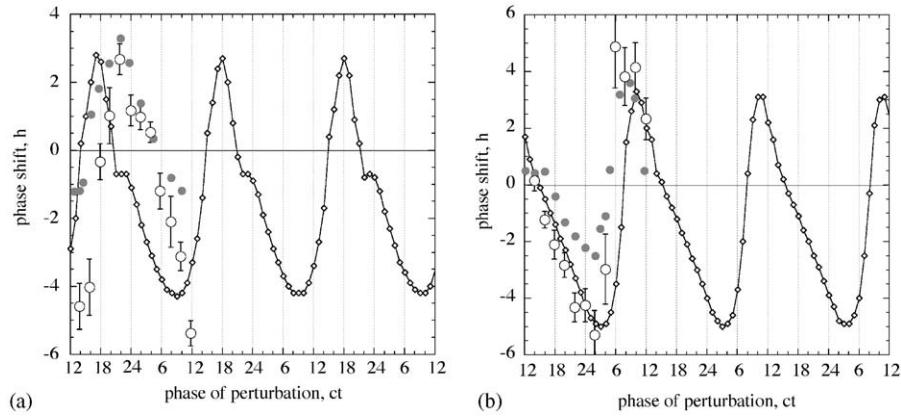


Fig. 8. Calculated phase response curves of (a) 12 h high (20 °C → 28 °C) and (b) 12 h low (28 °C → 20 °C) temperature pulses on the temperature compensated model (*per*⁺ parametrization, Table 5). Prior to the applied temperature pulse the oscillator was entrained to 11.25:11.25 L/D cycles at (a) 20 °C or (b) 28 °C. During the light phases the degradation rate constant k_{16} of PER/TIM were increased by 0.05 h⁻¹. The 12 h temperature pulses were then applied at different phases in darkness for a 72 h period after the final LD → DD transition, which defines the phase as ct 12. Experimental results by Zimmerman et al. (1968) and Chandrashekar (1974) are redrawn as gray dots and open circles, respectively.

oscillations and their robustness may be enhanced (Kurosawa and Iwasa, 2002; Kurosawa et al., 2002), which will probably also be the case in the present model. In fact, in many of the recent models of the *Drosophila* or mammalian circadian clocks (Goldbeter, 2002; Gonze et al., 2000; Leloup and Goldbeter, 1998, 2000, 2003; Smolen et al., 2001), Michaelis–Menten type kinetics have been included. However, whether Michaelis–Menten kinetic terms are essential in circadian time keeping mechanisms is yet to be understood.

Although the relative phases of *dClk*-mRNA, and PDP1 and VRI proteins match experimental findings (Figs. 2b, c), there are also some significant discrepancies between model and experiment. For example in the first part of the cycle where experiment (Fig. 2c) shows a low and slowly increasing PDP1 concentration, the calculations show that PDP1 values rapidly decrease and reach a steep minimum (Fig. 2b). Further, the experimental data demonstrate (Cyran et al., 2003; Glossop et al., 2003) that VRI is in antiphase compared to *dClk*-mRNA, while calculations suggest that the VRI maximum occurs slightly before the *dClk*-mRNA minimum (Figs. 2b, c). These phase behavior properties of the model were quite rigid indicating that certain phase determining aspects between PDP1, VRI and *dClk* might still be missing.

4.2. Influence of PDP1-positive feedback on properties on the oscillation

The observation that the expression of *per/tim* acts as part of an amplifier, with the *Pdp1*-positive feedback loop as the source of the oscillator’s amplification and stabilization (Fig. 3) assigns a new putative function for PER/TIM and the *Pdp1*-positive feedback loop to the *Drosophila* circadian clock. This result is in contrast to the findings that in oscillator models consisting of

positive and negative feedback loops with time delays, the positive feedback was not found crucial for the oscillations (Smolen et al., 2001, 2002, 2004). This discrepancy may be due to the fact that delay terms alone can generate oscillations. Consider the following sequence of first-order reactions



where the appearance of X_N is delayed by a certain time interval τ compared with the disappearance of X_0 . In reaction kinetics it is well established that process S1 will not be able to show sustained oscillations (Higgins, 1967). However, by representing the disappearance/appearance of X_0 , X_N as a process of the form



described by the delay equations

$$\frac{dX_N}{dt}(t) = kX_0(t - \tau), \quad (20a)$$

$$\frac{dX_0}{dt}(t) = -kX_0(t - \tau) \quad (20b)$$

and the mass balance

$$\frac{dX_N}{dt} + \frac{dX_0}{dt} = 0 \quad (20c)$$

oscillations in X_0 and X_N can be observed when τ is suitably chosen (for example for $\tau = \pi/2$ time units the solution becomes oscillatory $X_0(t) = \sin(kt)$ or $X_0(t) = \cos(kt)$), opposite to what is expected from the non-oscillatory behavior of process S1. This suggests that it may not be unproblematic to approximate/simplify chemical rate equations by delay equations. Furthermore, the time discontinuity in the system imposed by Eqs. (20) leads to a concentration discontinuity. As X_0 is not defined for $t < t_0$ (because then $X_0(t_0)$ would not be an initial value) one has to assume that the

time discontinuity of Eq. (20) applies for $t \geq t_0 + \tau$. By assuming this, $X_0(t)$ (Eq. 20b) becomes periodically discontinuous (with a period of τ), leading to oscillations in X_0 . While differential equations with delay terms are used in modeling circadian rhythms (Johnsson and Karlsson, 1972; Johnsson et al., 1973; Lewis, 1994), their application in reaction kinetic models (Epstein, 1990) appears to be unclear and implications on the importance of the positive feedback loops (Smolen et al., 2002, 2004) may be blurred by potential artefacts that may be generated in (chemically unrealistic) delay equations. In summary, the issue related to the usage of delay equations leading to possible artefacts needs a more careful analysis. In a personal communication Dr. P. Smolen informed us that in the Smolen et al. (2004) model circadian oscillations are preserved when the time delay (with or without positive feedback) is removed.

4.3. Effect of gene dosages

With a single negative feedback model, such as the Goodwin oscillator (Goodwin, 1965) the effect of *per* dosage was difficult to model, because all synthesis reactions within the negative feedback loop have positive C_i^P values (Ruoff and Rensing, 1996). With the coupling of the *per/tim* expression to the *Pdp1* and *vri* feedback loops (the “amplifier”, Fig. 1), the effect of *per* dosage can be modeled by assuming a power-law relationship between the rate constant of transcription (k_7) and the *per/tim* dosage (Eq. (15), Fig. 3a). Transcription/translation involves many proteins and processes (Alberts et al., 2002) and Eq. (15) is an empirical relationship between the gene dosage and the assignment of a single rate constant to those processes. In chemical kinetics such empirical power law relationships (reaction orders) are often used when the molecular mechanism for a process is unknown (Laidler and Meiser, 1995).

4.4. Temperature compensation, PER/TIM and PER/TIM dCLK CYC stabilities

Temperature compensation and other homeostatic regulation of the circadian period (Pittendrigh and Caldarola, 1973; Ruoff et al., 2000) are important clock properties. Temperature compensation is observed although many, if not all, of the underlying component processes are considered to have Q_{10} values of about 2–3 (“Van’t Hoff’s rule”). To obtain temperature compensation for a reaction kinetic oscillator model, some of the C_i^P ’s need to be *positive* such that Eq. (18) is fulfilled and positive and negative contributions balance each other within a certain temperature range. The possibility that temperature compensation may be understood in terms of such opposing reactions was already suggested

in the late 1950 (Hastings and Sweeney, 1957), and is considered to be a latent property found in any reaction kinetic oscillator (Ruoff, 1992). In the temperature compensated set describing *per*⁺ (Table 5), we found that some of the stochastically selected E_i values were quite low (for example E_{16} for the PER/TIM degradation). This may suggest that for some of the processes (such as the PER/TIM degradation) additional compensation mechanisms may come into play to ensure such a low activation energy. Additional mechanisms may be the “instantaneous compensation”, which has been observed for Michaelis–Menten type kinetics or diffusion controlled processes (Andjus et al., 2002; Ruoff et al., 2000). In instantaneous temperature compensation, the K_M and V_{\max} values of an enzyme-catalysed process increase both with temperature such that the overall reaction becomes independent of temperature (Andjus et al., 2002). In diffusion controlled processes the reactions are so fast that the transport of reactants by diffusion becomes the rate limiting step. In the latter case reactions depend little on temperature, but viscosity changes of the reaction medium (cytoplasm) due to temperature variations have normally the largest impact on diffusion controlled reactions. One may even speculate whether the cell may have evolved mechanisms which can keep the viscosity of the cytosol constant at different temperatures to ensure that reaction rates of diffusion controlled processes become independent of temperature. However, it should also be noted that compared to the cellular dimensions, diffusion of (clock) proteins is a fairly rapid process, hence diffusion is generally not a rate limiting step in the generation of circadian rhythms (Winfree, 2000).

As already predicted in an earlier study on the Goodwin oscillator (Ruoff et al., 1996) the temperature response behavior of *per*^S mutants can be obtained by decreasing the PER protein stability (i.e. by increasing k_{16}) and making the degradation of PER/TIM more temperature sensitive by increased E_{16} values (Table 5). We are not aware of any experiment, which has measured the turnover of PER^S compared to PER⁺.

In describing the *per*^L mutant, the largest change needed in our model compared to *per*⁺ is a reduction of k_{17} , which suggests that the binding between PER/TIM and dCLK_n (Bae et al., 2000; Lee et al., 1999) should be weakened in *per*^L mutants (Table 5). It was previously shown that *per*^L contains a point mutation within its PAS domain, which seems to be of importance for the PER/TIM–dCLK interaction and the formation of PER dimers. Alternatively, the PAS domain of PER can interact intramolecularly with another domain within PER. Both intra- and intermolecular interactions have been suggested to be of importance for *Drosophila*’s temperature compensation (Huang et al., 1995).

4.5. Influence of light and temperature pulse PRCs

In order to model temperature pulse PRCs we used the temperature compensated per^+ parametrization (Table 5) and, as in the Zimmerman et al. (1968) experiments, first entrained the oscillator to light dark cycles at 20 or 28 °C, before 12 h dark HTPs or LTPs (20→28 °C or 28→20 °C) were applied (Fig. 8). However, to our surprise, the oscillator entrained to L/D cycles only within a very small window near its natural period. The reason for such “rigidity” of the oscillator towards L/D cycles seems to be that the influence of light is represented by only one reaction, i.e. by an increased degradation of PER/TIM. On the other hand, when analysing temperature entrainment of the temperature compensated oscillator, the oscillator seems to entrain more easily and to a wider range of T -cycles (data not shown). We wish to return to the question which factors influence/enhance the entrainment of a biological oscillator by L/D or temperature cycles in a later study.

However, when entrainment by L/D cycles does occur in the model, the phase of PER/TIM is dependent upon the rate of PER/TIM degradation during the light phase (Fig. 7). It was recently shown (Bao et al., 2001) that under 12:12 h L/D cycles the phase of PER is delayed in per^S mutants relative to PER in per^+ flies. The results described in Fig. 7 indicate that a delayed appearance of PER as in per^S (Fig. 7c) may be due to a diminished light-induced degradation of PER (Fig. 7d). Because the model suggests that PER^S degradation is already increased in darkness compared to PER^+ degradation (Table 5), light may have a smaller effect on PER^S degradation than on PER^+ degradation, and therefore could lead to a delay in the appearance of the PER peak in per^S . Furthermore, the reduced maximum level of PER in per^S compared to per^+ can be accounted for by the generally increased degradation of PER in per^S flies both under light or dark conditions (Fig. 6b).

The calculated PRCs of temperature pulse perturbations (Fig. 8) closely match the classical experiments by Zimmerman et al. (1968) and Chandrashekar (1974). The reason why there is a slightly better agreement between experimental and simulated PRCs for the LTP case (28→20 °C, Fig. 8b) is not clear. However, additional calculations showed that altered temperature levels during the prior L/D cycles may lead to a better match between experimental and simulated data (data not shown). Another aspect, which we found interesting and that might be worth investigating in a later study is how a temperature PRC may vary due to changes in activation energies, while keeping temperature compensation intact.

4.6. Oscillations in PER-less mutants

As seen from the results in Fig. 3, the interlocking-feedback loop model offers the possibility of “core” self

sustained oscillations even in the absence of per/tim . However, even under such conditions $dClk$ should be still an essential oscillator element. In a related model of the mammalian circadian clock which was lacking PER protein oscillations could still be observed (Leloup and Goldbeter, 2003, 2004).

There have been several reports indicating oscillations may occur in fly strains that lack functional per (Dowse and Ringo, 1987; Helfrich and Engelmann, 1987; Helfrich-Förster, 2001; Yoshii et al., 2002). Experimental data often show a lengthening of the period for per^0 flies that are still rhythmic. This is also observed in our model (data not shown) and is consistent with the model’s description of per dosage effects (Fig. 5a).

By using a time series technique, Dowse and Ringo (1987) analysed the signal-to-noise ratio (SNR) of locomotor activities in per^+ , per^S , per^L and per^0 strains. They found that ultradian rhythm components are present in per^0 flies, and that the SNR increased significantly in the presence of per , which indicates that PER indeed acts as an amplifier (Fig. 3a, b). Helfrich and Engelmann (1987) found that the range of L/D entrainment in per^0 flies is significantly narrowed compared to per^+ flies, and that per^0 flies are capable of generating endogenous oscillations. They concluded that the per gene product is necessary as a normal output of the clock controlling locomotor activity, but that per is not concerned with the central clock structure. Helfrich-Förster (2001) found evidence for a two oscillator system (described as morning and evening oscillators) in which the morning oscillator is assumed to track light. Two reports recently showed that the morning and evening locomotor behavior of *Drosophila* is controlled by per by using coupled but different clock neurons (Grima et al., 2004; Stoleru et al., 2004).

By applying periodic temperature cycles on a variety of mutants, Yoshii et al. (2002) found evidence that per -less flies still have a weak oscillatory mechanism, which seem to require $dClk$ and cyc . Our results that the model is poorly entrained by L/D cycles may indicate that part of the circadian light tracking system is incomplete in the model and that the “core” may contain additional light mediating properties and feedback loops which would enhance the sensitivity of the model to L/D cycles. These aspects will be considered in a future study on an extended variant of the interlocking-feedback loop model.

Acknowledgments

We thank Ludger Rensing, Paul Smolen, Anders Johnsson and Chris Hong for comments on the manuscript, Theodor Ivesdal for UNIX help, and the University of Stavanger for financial support to MKC and travel funds for VKS.

References

- Alberts, B., Johnson, A., Lewis, J., Raff, M., Roberts, K., Walter, P., 2002. Molecular Biology of the Cell, Fourth ed. Garland Science, New York.
- Andjus, R.K., Dzakula, Z., Marjanovic, M., Zivadinovic, D., 2002. Kinetic properties of the enzyme-substrate system: a basis for immediate temperature compensation. *J. Theor. Biol.* 217 (1), 33–46.
- Bae, K., Lee, C., Hardin, P.E., Edery, I., 2000. dCLOCK is present in limiting amounts and likely mediates daily interactions between the dCLOCK-CYC transcription factor and the PER-TIM complex. *J. Neurosci.* 20 (5), 1746–1753.
- Bao, S., Rihel, J., Bjes, E., Fan, J.Y., Price, J.L., 2001. The *Drosophila* double-timeS mutation delays the nuclear accumulation of period protein and affects the feedback regulation of period mRNA. *J. Neurosci.* 21 (18), 7117–7126.
- Blau, J., Young, M.W., 1999. Cycling vrille expression is required for a functional *Drosophila* clock. *Cell* 99 (6), 661–671.
- Bünning, E., 1963. The Physiological Clock. Springer, Berlin.
- Chandrashekar, M.K., 1974. Phase Shifts in the *Drosophila pseudoobscura* circadian rhythm evoked by temperature pulses of varying durations. *J. Interdiscipl. Cycle Res.* 5, 371–380.
- Cote, G.G., Brody, S., 1986. Circadian rhythms in *Drosophila melanogaster*: analysis of period as a function of gene dosage at the per (period) locus. *J. Theor. Biol.* 121 (4), 487–503.
- Cyran, S.A., Buchsbaum, A.M., Reddy, K.L., Lin, M.C., Glossop, N.R., Hardin, P.E., Young, M.W., Storti, R.V., Blau, J., 2003. vrille, Pdp1, and dClock form a second feedback loop in the *Drosophila* circadian clock. *Cell* 112 (3), 329–341.
- Dixon, M., Webb, E.C., Thorne, C.J.R., Tipton, K.F., 1979. Enzymes. Longman, London.
- Dowse, H.B., Ringo, J.M., 1987. Further evidence that the circadian clock in *Drosophila* is a population of coupled ultradian oscillators. *J. Biol. Rhythms* 2, 65–76.
- Dunlap, J.C., 1999. Molecular bases for circadian clocks. *Cell* 96 (2), 271–290.
- Dunlap, J.C., Loros, J.J., DeCoursey, P.J., 2003. Biological Time-keeping. Sinauer Associates, Inc. Publishers, Sunderland.
- Edmunds, L.N., 1988. Cellular and Molecular Bases of Biological Clocks. Springer, New York.
- Epstein, I.R., 1990. Differential delay equations in chemical kinetics: some simple linear model systems. *J. Chem. Phys.* 92, 1702–1712.
- Feldman, J.F., Hoyle, M.N., 1973. Isolation of circadian clock mutants of *Neurospora crassa*. *Genetics* 75 (4), 605–613.
- Forger, D.B., Peskin, C.S., 2003. A detailed predictive model of the mammalian circadian clock. *Proc. Natl Acad. Sci. USA* 100 (25), 14806–14811.
- Franck, U.F., 1980. Feedback kinetics in physicochemical oscillators. *Ber. Bunsenges. Phys. Chem.* 84, 334–341.
- Froehlich, A.C., Pregueiro, A., Lee, K., Denault, D., Colot, H., Nowrousian, M., Loros, J.J., Dunlap, J.C., 2003. The molecular workings of the *Neurospora* biological clock. *Novartis Found Symp.* 253, 184–198 discussion 102–9, 198–202, 281–4.
- Glossop, N.R., Houl, J.H., Zheng, H., Ng, F.S., Dudek, S.M., Hardin, P.E., 2003. VRILLE feeds back to control circadian transcription of Clock in the *Drosophila* circadian oscillator. *Neuron* 37 (2), 249–261.
- Goldbeter, A., 2002. Computational approaches to cellular rhythms. *Nature* 420 (6912), 238–245.
- Gonze, D., Leloup, J.C., Goldbeter, A., 2000. Theoretical models for circadian rhythms in *Neurospora* and *Drosophila*. *C. R. Acad. Sci. III* 323 (1), 57–67.
- Goodwin, B.C., 1965. Oscillatory Behavior in Enzymatic Control Processes, vol. 3. Pergamon Press, Oxford, pp. 425–438.
- Grima, B., Chelot, E., Xia, R., Rouyer, F., 2004. Morning and evening peaks of activity rely on different clock neurons of the *Drosophila* brain. *Nature* 431 (7010), 869–873.
- Hastings, J.W., Sweeney, B.M., 1957. On the mechanism of temperature independence in a biological clock. *Proc. Natl Acad. Sci. USA* 43, 804–811.
- Heinrich, R., Schuster, S., 1996. The Regulation of Cellular Systems. Chapman & Hall, New York.
- Helfrich, C., Engelmann, W., 1987. Evidences for circadian rhythmicity in the *per*⁰ mutant of *Drosophila melanogaster*. *Z. Naturforsch.* 42c, 1335–1338.
- Helfrich-Förster, C., 2001. The locomotor activity rhythm of *Drosophila melanogaster* is controlled by a dual oscillator system. *J. Insect Physiol.* 47, 877–887.
- Higgins, J., 1967. The theory of oscillating reactions. *Ind. Eng. Chem.* 59, 18–62.
- Hong, C.I., Tyson, J.J., 1997. A proposal for temperature compensation of the circadian rhythm in *Drosophila* based on dimerization of the PER protein. *Chronobiol. Int.* 14 (5), 521–529.
- Huang, Z.J., Curtin, K.D., Rosbash, M., 1995. PER protein interactions and temperature compensation of a circadian clock in *Drosophila*. *Science* 267 (5201), 1169–1172.
- Hunter-Ensor, M., Ousley, A., Sehgal, A., 1996. Regulation of the *Drosophila* protein timeless suggests a mechanism for resetting the circadian clock by light. *Cell* 84 (5), 677–685.
- Johnsson, A., Karlsson, H.G., 1972. A feedback model for biological rhythms. *J. Theor. Biol.* 36, 153–174.
- Johnsson, A., Karlsson, H.G., Engelmann, W., 1973. Phase-shift effects in *Kalanchoë* petal rhythm due to 2 or more light pulses. Theoretical and experimental study. *Physiol. Plantarum* 28, 134–142.
- Klarsfeld, A., Leloup, J.C., Rouyer, F., 2003. Circadian rhythms of locomotor activity in *Drosophila*. *Behav. Process.* 64 (2), 161–175.
- Konopka, R.J., Benzer, S., 1971. Clock mutants of *Drosophila melanogaster*. *Proc. Natl Acad. Sci. USA* 68 (9), 2112–2116.
- Konopka, R.J., Pittendrigh, C., Orr, D., 1989. Reciprocal behaviour associated with altered homeostasis and photosensitivity of *Drosophila* clock mutants. *J. Neurogenet.* 6 (1), 1–10.
- Kóvacs, K.M., Rábai, G., 2002. Temperature-compensation in pH-oscillators. *Phys. Chem. Chem. Phys.* 4, 5265–5269.
- Kurosawa, G., Iwasa, Y., 2002a. Saturation of enzyme kinetics in circadian clock models. *J. Biol. Rhythms* 17, 568–577.
- Kurosawa, G., Mochizuki, A., Iwasa, Y., 2002b. Comparative study of circadian clock models, in search of processes promoting oscillation. *J. Theor. Biol.* 216, 193–208.
- Laidler, K.J., Meiser, J.H., 1995. Physical Chemistry, Second ed. Houghton Mifflin Company, Geneva (Illinois).
- Lakin-Thomas, P.L., Brody, S., Cote, G.G., 1991. Amplitude model for the effects of mutations and temperature on period and phase resetting of the *Neurospora* circadian oscillator. *J. Biol. Rhythms* 6 (4), 281–297.
- Lee, C., Bae, K., Edery, I., 1999. PER and TIM inhibit the DNA binding activity of a *Drosophila* CLOCK-CYC/dBMAL1 heterodimer without disrupting formation of the heterodimer: a basis for circadian transcription. *Mol. Cell Biol.* 19 (8), 5316–5325.
- Lee, C., Parikh, V., Itsukaichi, T., Bae, K., Edery, I., 1996. Resetting the *Drosophila* clock by photic regulation of PER and a PER-TIM complex. *Science* 271 (5256), 1740–1744.
- Lee, K., Loros, J.J., Dunlap, J.C., 2000. Interconnected feedback loops in the *Neurospora* circadian system. *Science* 289 (5476), 107–110.
- Leloup, J.C., Goldbeter, A., 1998. A model for circadian rhythms in *Drosophila* incorporating the formation of a complex between the PER and TIM proteins. *J. Biol. Rhythms* 13 (1), 70–87.
- Leloup, J.C., Goldbeter, A., 1999. Chaos and birhythmicity in a model for circadian oscillations of the PER and TIM proteins in *Drosophila*. *J. Theor. Biol.* 198 (3), 445–459.

- Leloup, J.C., Goldbeter, A., 2000. Modeling the molecular regulatory mechanism of circadian rhythms in *Drosophila*. *Bioessays* 22 (1), 84–93.
- Leloup, J.C., Goldbeter, A., 2003. Toward a detailed computational model for the mammalian circadian clock. *Proc. Natl Acad. Sci. USA* 100 (12), 7051–7056.
- Leloup, J.C., Goldbeter, A., 2004. Modeling the mammalian circadian clock: sensitivity analysis and multiplicity of oscillatory mechanisms. *J. Theor. Biol.* 230 (4), 541–562.
- Lewis, R.D., 1994. Modelling the circadian system of the weta, *Hemideina thoracica* (Orthoptera: Stenopelmatidae). *J. R. Soc. New Zealand* 24, 395–421.
- Lillo, C., Ruoff, P., 1984. A minimal oscillator model of light-induced circadian rhythms in leaves of barley. *Physiol. Plantarum* 62, 589–592.
- Liu, Y., Loros, J., Dunlap, J.C., 2000. Phosphorylation of the *Neurospora* clock protein FREQUENCY determines its degradation rate and strongly influences the period length of the circadian clock. *Proc. Natl Acad. Sci. USA* 97 (1), 234–239.
- Luttge, U., 2000. The tonoplast functioning as the master switch for circadian regulation of crassulacean acid metabolism. *Planta* 211 (6), 761–769.
- Myers, M.P., Wager-Smith, K., Rothenfluh-Hilfiker, A., Young, M.W., 1996. Light-induced degradation of TIMELESS and entrainment of the *Drosophila* circadian clock. *Science* 271 (5256), 1736–1740.
- Nagy, G., Körös, E., Oftedal, N., Tjellflaat, K., Ruoff, P., 1996. Effect of temperature in cerium-ion-catalyzed bromate-driven oscillators. *Chem. Phys. Lett.* 250, 255–260.
- Neff, R., Blasius, B., Beck, F., Luttge, U., 1998. Thermodynamics and energetics of the tonoplast membrane operating as a hysteresis switch in an oscillatory model of Crassulacean acid metabolism. *J. Membr. Biol.* 165 (1), 37–43.
- Pittendrigh, C.S., 1993. Temporal organization: reflections of a Darwinian clock-watcher. *Ann. Rev. Physiol.* 55, 16–54.
- Pittendrigh, C.S., Caldarola, P.C., 1973. General homeostasis of the frequency of circadian oscillations. *Proc. Natl Acad. Sci. USA* 70 (9), 2697–2701.
- Preuss, F., Fan, J.Y., Kalive, M., Bao, S., Schuenemann, E., Bjes, E.S., Price, J.L., 2004. *Drosophila* doubletime mutations which either shorten or lengthen the period of circadian rhythms decrease the protein kinase activity of casein kinase I. *Mol. Cell Biol.* 24 (2), 886–898.
- Rábai, G., Hanazaki, I., 1999. Temperature compensation in the oscillatory hydrogen peroxide-thiosulfate-sulfite flow system. *Chem. Comm.*, 1965–1966.
- Radhakrishnan, K., Hindmarsh, A.C., 1993. Description and Use of LSODE, the Livermore Solver for Ordinary Differential Equations. National Aeronautics and Space Administration, Lewis Research Center, NASA Reference Publication 1327, Cleveland, OH, 44135-3191.
- Rensing, L., Ruoff, P., 2002. Temperature effect on entrainment, phase shifting, and amplitude of circadian clocks and its molecular bases. *Chronobiol. Int.* 19 (5), 807–864.
- Rosbash, M., Allada, R., McDonald, M., Peng, Y., Zhao, J., 2003. Circadian rhythms in *Drosophila*. *Novartis Found Symp.* 253, 223–232 discussion 52–5, 102–9, 232–7 passim.
- Ruoff, P., 1992. Introducing temperature-compensation in any reaction kinetic oscillator model. *J. Interdiscipl. Cycle Res.* 23, 92–99.
- Ruoff, P., 1995. Antagonistic balance in the Oregonator: About the possibility of temperature-compensation in the Belousov–Zhabotinsky reaction. *Physica D* 84, 204–211.
- Ruoff, P., Christensen, M.K., Wolf, J., Heinrich, R., 2003. Temperature dependency and temperature-compensation in a model of yeast glycolytic oscillations. *Biophys. Chem.* 106, 179–192.
- Ruoff, P., Mohsenzadeh, S., Rensing, L., 1996. Circadian rhythms and protein turnover: the effect of temperature on the period lengths of clock mutants simulated by the Goodwin oscillator. *Naturwissenschaften* 83 (11), 514–517.
- Ruoff, P., Rensing, L., 1996. The temperature-compensated Goodwin model simulates many circadian clock properties. *J. Theor. Biol.* 179, 275–285.
- Ruoff, P., Vinsjevik, M., Mohsenzadeh, S., Rensing, L., 1999a. The Goodwin model: simulating the effect of cycloheximide and heat shock on the sporulation rhythm of *Neurospora crassa*. *J. Theor. Biol.* 196 (4), 483–494.
- Ruoff, P., Vinsjevik, M., Monnerjahn, C., Rensing, L., 1999b. The Goodwin oscillator: on the importance of degradation reactions in the circadian clock. *J. Biol. Rhythms* 14 (6), 469–479.
- Ruoff, P., Vinsjevik, M., Monnerjahn, C., Rensing, L., 2001. The Goodwin model: simulating the effect of light pulses on the circadian sporulation rhythm of *Neurospora crassa*. *J. Theor. Biol.* 209 (1), 29–42.
- Ruoff, P., Vinsjevik, M., Rensing, L., 2000. Temperature compensation in biological oscillators: a challenge for joint experimental and theoretical analysis. *Comments Theor. Biol.* 5, 361–382.
- Smith, R.F., Konopka, R.J., 1982. Effects of dosage alterations at the *per* locus on the period of the circadian clock of *Drosophila*. *Mol. Gen. Genet.* 185, 30–36.
- Smolen, P., Baxter, D.A., Byrne, J.H., 2001. Modeling circadian oscillations with interlocking positive and negative feedback loops. *J. Neurosci.* 21 (17), 6644–6656.
- Smolen, P., Baxter, D.A., Byrne, J.H., 2002. A reduced model clarifies the role of feedback loops and time delays in the *Drosophila* circadian oscillator. *Biophys. J.* 83 (5), 2349–2359.
- Smolen, P., Baxter, D.A., Byrne, J.H., 2003. Reduced models of the circadian oscillators in *Neurospora crassa* and *Drosophila melanogaster* illustrate mechanistic similarities. *Omics* 7 (4), 337–354.
- Smolen, P., Hardin, P.E., Lo, B.S., Baxter, D.A., Byrne, J.H., 2004. Simulation of *Drosophila* circadian oscillations, mutations, and light responses by a model with VRI, PDP-1, and CLK. *Biophys. J.* 86 (5), 2786–2802.
- Stoleru, D., Peng, Y., Agosto, J., Rosbash, M., 2004. Coupled oscillators control morning and evening locomotor behaviour of *Drosophila*. *Nature* 431 (7010), 862–868.
- Tyson, J.J., Hong, C.I., Thron, C.D., Novak, B., 1999. A simple model of circadian rhythms based on dimerization and proteolysis of PER and TIM. *Biophys. J.* 77 (5), 2411–2417.
- Ueda, H.R., Hagiwara, M., Kitano, H., 2001. Robust oscillations within the interlocked feedback model of *Drosophila* circadian rhythm. *J. Theor. Biol.* 210 (4), 401–406.
- Winfree, A.T., 2000. The geometry of biological time, Second ed. Springer, New York.
- Yoshii, T., Sakamoto, M., Tomioka, K., 2002. A temperature-dependent timing mechanism is involved in the circadian system that drives locomotor rhythms in the fruit fly *Drosophila melanogaster*. *Zoolog. Sci.* 19 (8), 841–850.
- Young, M.W., Wager-Smith, K., Vosshall, L., Saez, L., Myers, M.P., 1996. Molecular anatomy of a light-sensitive circadian pacemaker in *Drosophila*. *Cold Spring Harb. Symp. Quant. Biol.* 61, 279–284.
- Yu, Q., Jacquier, A.C., Citri, Y., Hamblen, M., Hall, J.C., Rosbash, M., 1987. Molecular mapping of point mutations in the period gene that stop or speed up biological clocks in *Drosophila melanogaster*. *Proc. Natl Acad. Sci. USA* 84 (3), 784–788.
- Zeng, H., Qian, Z., Myers, M.P., Rosbash, M., 1996. A light-entrainment mechanism for the *Drosophila* circadian clock. *Nature* 380 (6570), 129–135.
- Zimmerman, W.F., Pittendrigh, C.S., Pavlidis, T., 1968. Temperature compensation of the circadian oscillation in *Drosophila pseudoobscura* and its entrainment by temperature cycles. *J. Insect Physiol.* 14 (5), 669–684.